Enhanced triboelectric nanogenerator performance via an optimised low permittivity, low thickness substrate

Guanbo Min, Libu Manjakkal, Daniel M. Mulvihill and Ravinder S. Dahiya
School of Engineering, University of Glasgow, Glasgow, G12 8QQ, U.K.
Ravinder.Dahiya@glasgow.ac.uk

***Abstract*—With electrical power generated from mechanical contact, the triboelectric nanogenerators (TENGs) have attracted attention recently as a promising route to realising self-powered sensors (e.g. tactile sensors, biomedical sensors etc.). Due to their limited power range (0.1-100 mW/cm^2), it is important to optimise the output performance of TENGs. Among the factors that confer higher performance are materials with a strong triboelectric effect and materials with low permittivity. It can be difficult to realize these two benefits in a single contact material. This paper presents a solution to this challenge by optimising a low permittivity substrate beneath the tribo-contact layer. Results are simulated over a range of both substrate permittivity and thickness. The open circuit voltage is found to increase by a factor of 1.8 in moving from PVDF to the lower permittivity PTFE and by a further factor of 37.2 when the substrate thickness is reduced from 200 to 1 µm. For PTFE with 1 µm thickness, this amounts to 12.2 kV, as against 327V known from simulations up to now. These results clearly indicate that optimized low permittivity, low thickness substrates represent a potential route to self-powered sensors.**

Keywords—Triboelectric nanogenerator; Self-powered Sensors; Permittivity; Dielectric;

I. INTRODUCTION

Energy autonomy is key to the acceptance of next generation portable and wearable systems that are being offered for several applications such as health monitoring [1-4], robotics [5-8] as well as other micro/nano sensors systems that are being developed for environment monitoring [9] and internet of things (IoT) applications. Currently, the energy requirements of these sensor systems are met with bulky batteries, energy storage devices such as supercapacitors, and energy harvesters that do not always produce required energy. Because of this, significant efforts have been devoted during recent decades to develop alternative solutions such as light-weight and wearable energy harvesters based on photovoltaics [10], thermo-electricity [11], piezo-electricity [12] and tribo-electricity [13] etc. The latter is particularly attractive as it allows generation of power from flexible or wearable substrates that are used for integration of sensors [14]. The triboelectric nanogenerators (TENGs) offer high efficiency, are less complex and are cost-effective. It is possible to used triboelectricity in conjunction with other energy harvesters, for example, with photovoltaics [15,16]. Further, it is possible to use this method to generate energy for wearable systems from daily movements such as walking etc [17].

TENGs produce electrical energy via a combination of triboelectric effect and electrostatic induction [18]. When two surfaces contact each other, tribo-charges can be transferred between them due to differences in work function and electronegativity of the contacting materials [19-24]. The tribo-charges that develop on two interface surfaces generate an electric field and are the energy source for the generation of output voltage and current [25-27]. For optimum performance, materials with a strong triboelectric effect and materials with low permittivity within the bulk are required [18]. However, the majority of triboelectric materials will not confer both optimum triboelectric effect and low permittivity. For example, PVDF is a strongly negative triboelectric material, because of the high work function of the fluorine atoms. However, PVDF has a high permittivity which is not optimum. An in-depth study is needed to evaluate the interplay between such material properties to obtain TENGs with optimum performance. This is important considering the current gap between the limited power (~0.1-100 mW/cm^2) available from TENGs [28] and the power needed to develop self-powered sensors and electronics (8.44-107mW/m^2) [29]. In this regard, this paper presents a study on optimising a low permittivity substrate below the tribo-contact surface so that gains from both the triboelectric effect and the low permittivity can be harnessed.

This paper implements a low permittivity substrate (yellow layer in Fig. 1) and simulates the effect of varying both substrate permittivity and thickness upon TENG output metrics such as open circuit voltage, short circuit charge density and short circuit current density. Reducing both the substrate permittivity and thickness was found to increase open circuit voltage by a factor of 37.2. While reducing substrate permittivity had little effect on short circuit current and charge density, reducing substrate thickness does significantly increase these.

This paper is organized as follows: the equivalent relative permittivity of tribo-layer with different substrates are calculated in section II, the output results with different substrates and thickness of PTFE are discussed in section III. Finally, the concluding section IV summarizes the key results and consideration of future work.

II. SIMULATION EXPERIMENT

The TENG consists of two contacting layers (‘Layer 1’ and ‘Layer 2’) comprising a parallel plate capacitor as shown in

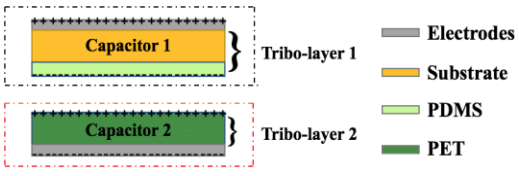

Figure 1. Contact mode ‘TENG’ with low permittivity ‘substrate’.

This work was partially supported by EPSRC Engineering Fellowship for Growth under Grant (EP/M002527/1), UK.

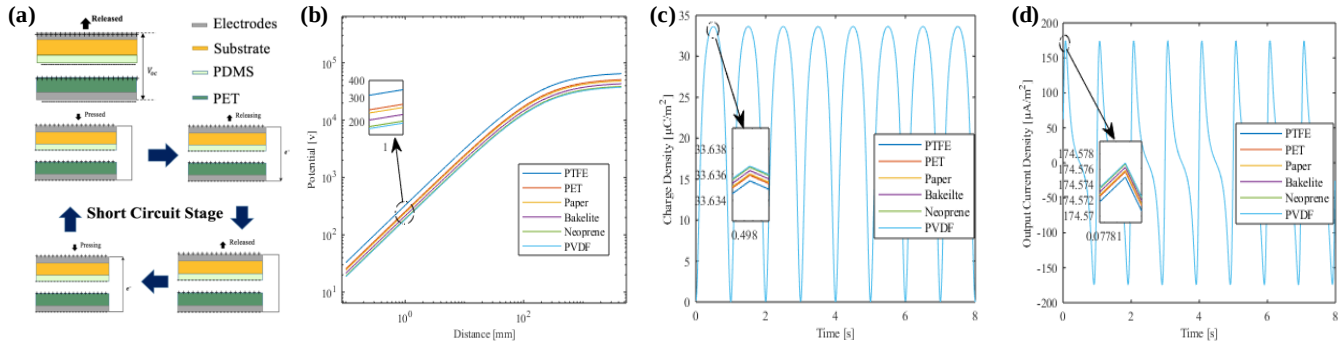

Figure 2. (a) Contact mode dielectric-dielectric TENG at open circuit and short circuit configurations and the outputs: (b) Open circuit voltage (c) Short circuit charge density and (d) Short circuit current density with substrate materials having a range of permittivity values (at 1mm separation distance).

Table I. Parameters for triboelectric 'Layer 1'

Substrate	PDMS
Thickness ($d_1 = 200\mu m$)	Thickness ($d_2 = 20\mu m$)
Relative Permittivity (ε_{r1}) varying	Relative Permittivity ($\varepsilon_{r2} = 2.7$)
Areas for $25cm^2$	Areas for $25cm^2$

Table II. Equivalent relative permittivity ($\varepsilon_{r,eq}$) and equivalent permittivity (ε_{eq}) for triboelectric 'Layer1'.

Substrate Materials [23]	$\varepsilon_{r,eq}$ of tribo-'Layer 1'	ε_{eq} of tribo-'Layer1' $\times 10^{-12}$F/m
PTFE (Teflon)	2.1	18.9
PET	3.2	28.7
Paper	3.6	31.7
Bakelite	4.6	40.4
Neoprene Rubber	5.9	52.3
PVDF	6.5	57.2

Fig 1. Here, the permittivity and thickness of the dielectric are the two essential parameters that govern the output performance. The interface pair is nominally selected as PDMS and PET (as in Fig. 1) at the tribo-charge density of $40.7\mu C/m^2$ [30]. The output performances are then simulated for the TENG with different substrate permittivity and thicknesses using the distance-dependent electric field model [30, 31]. First, an optimum realistic material is decided based on optimum permittivity and then thickness is optimized using this material as the substrate. Based on the parameters in Table I, the total equivalent permittivity of triboelectric 'Layer 1' can be calculated by the parallel plate capacitor model. The capacitance of the substrate layer (in TENG 'Layer 1') is given by $C = \varepsilon A / d$ [32], where C is capacitance, ε is permittivity, d is thickness and A is the in-plane area. If the capacitance of triboelectric 'Layer 1' is supposed as two dielectrics in one capacitor, the equivalent capacitance of the two materials for triboelectric 'Layer 1' can be presented as:

$$\frac{1}{C_{eq}} = \frac{1}{C_1} + \frac{1}{C_2} \quad (1)$$

Where, C_1 and C_2 are the capacitances of PDMS and substrate respectively. Combining Eq. 1 and the formula for capacitance above, the equivalent permittivity for triboelectric 'Layer 1' is:

$$\varepsilon_{eq} = \frac{\varepsilon_{PDMS}\varepsilon_{Substrate}(d_{PDMS}+d_{Substate})}{d_{PDMS}\varepsilon_{Substrate}+d_{Substate}\varepsilon_{PDMS}} \quad (2)$$

Consequently, the equivalent permittivity of triboelectric 'Layer 1' with a range of different substrate materials (PTFE, PET, Paper, Bakelite, Neoprene rubber and PVDF) were calculated by Eq. 2. These are shown in Table II. These materials provide a reasonably wide range of permittivity. Therefore, the relationship between the relative permittivity and TENG output performances (including open voltage, short circuit charge density and short circuit current density) could be summarised by the results of simulations with these substrate materials. This allows determination of an optimum substrate material. In the second part of this work, the output performances have been compared at different thicknesses of the substrate (using the optimum substrate material) to obtain the advantageous structure for the TENGs.

III. Result and Discussion

Fig. 2(a) illustrates the cycle of interaction of the layered TENG, while Fig. 2(b-c) reports the device output (open circuit voltage vs separation distance, short circuit charge density vs time and short circuit current density vs time). Fig. 3 then plots these outputs explicitly against relative permittivity. It is clear from both Fig. 2(b) and Fig. 3(a) that open circuit voltage increases significantly as relative permittivity of tribo-layer 1 is reduced. For instance, in Fig. 3, the open circuit voltage increases from 184.8V to 327V (i.e. 1.8 times), when the substrate material changes from PVDF to PTFE (relative permittivity of tribo-layer 1 reduced from 6.5 to 2.1). Note, that the substrate is implanted under the negative triboelectric interface (PDMS) and a 1mm separation distance is used for these results. This improvement with PTFE can be 1.3 times the output reported in literature with PET (ε_r = 3.3) as the substrate material [30]. Hence, open circuit voltage can be enhanced by embedding a substrate with lower relative permittivity than the original triboelectric contact material to reduce the relative equivalent permittivity of the overall triboelectric layer ('Layer 1' in Fig. 1). Although Fig. 2(c-d) shows short circuit charge and current density declining somewhat with decreasing relative permittivity, Fig. 3(b) shows that the change is insignificant relative to the magnitudes of these outputs. Over the range of relative permittivity, they are approximately fixed at about 33.6 $\mu C/m^2$ and 174.6 $\mu A/m^2$ respectively. Hence, by choosing PTFE as the optimum substrate material, we can obtain useful increases in open circuit voltage while not affecting current and charge density very much.

Having selected PTFE as the substrate material, we now simulate how device output varies with substrate thickness. Separation height was again held constant at 1mm to compare the output performances at different thicknesses of substrate.

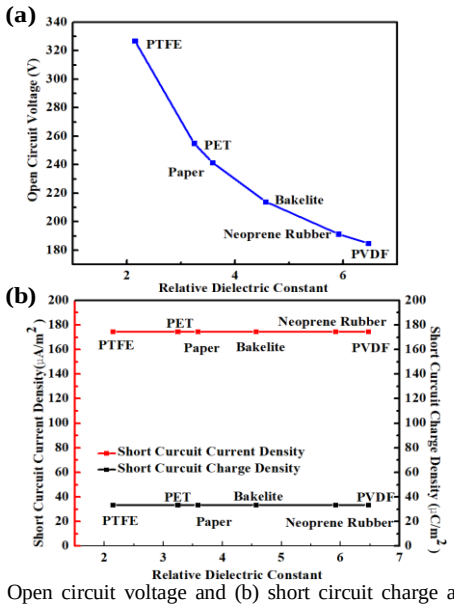

Figure 3. (a) Open circuit voltage and (b) short circuit charge and current densities versus relative permittivity for different substrate materials (at 1mm separation).

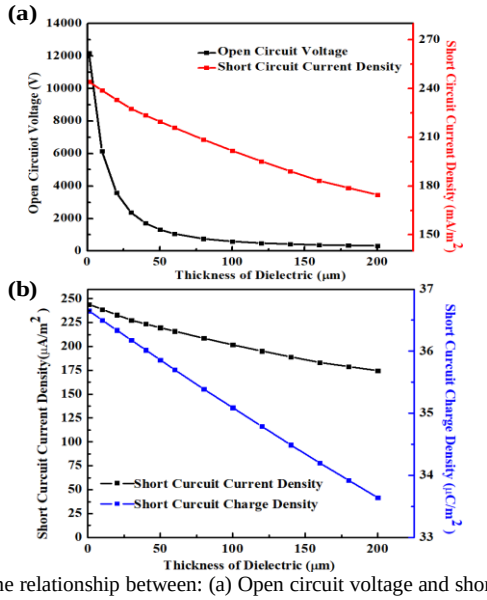

Figure 5. The relationship between: (a) Open circuit voltage and short circuit current density and (b) short circuit charge and current density at different thicknesses of PTFE (at 1mm separation).

Fig. 4 shows the resulting output performance (open circuit voltage vs separation distance, short circuit charge density vs time and short circuit current density vs time). Figs. 4 and 5 show that open circuit voltage, short circuit charge density and short circuit current density all increase significantly as the substrate thickness is reduced. In particular, the open circuit voltage at $1\mu m$ thickness of PTFE is approximately 37.2 times larger than the value at 200 μm thickness of PTFE. Simultaneously, the short circuit current density can be boosted to $69.5\mu A/m^2$ as shown in Fig. 5. Consequently, the simulation results have indicated that open circuit voltage, short circuit charge density and short circuit current density can all be improved significantly by implanting a low thickness, low permittivity material under the negative triboelectric interface.

IV. Conclusion

Materials with strong triboelectric effect and low permittivity are among the requirements for improving triboelectric nanogenerator (TENG) performance. These features are not always possible in the same material, so this paper outlines the idea of optimising a low permittivity substrate material underneath the tribo-contact layer so that both optimum triboelectric effect and low permittivity can be incorporated in the same TENG. Results (simulated using a distance-dependent electric field model [30, 31]) show that open circuit voltage increases with reducing substrate permittivity. Going from PVDF (ε_r =7.5) to PTFE (ε_r=2.1), open circuit voltage increased by a factor of 1.8. Therefore, PTFE was selected as a suitable substrate material. Over the same permittivity range, open circuit current and charge density were little affected. Finally, reducing the thickness of the substrate significantly increased open circuit voltage, and short circuit charge and current densities. In particular, reducing the substrate thickness of the PTFE substrate from 200 to 1 μm increased the open circuit voltage by approximately 37.2 times. Therefore, low permittivity, low thickness substrates can be used to boast TENG performance. Followed by this simulation work, the next aim is the fabrication of this TENG (for example by using PDMS with 1 μm thick substrate of PTFE and graphene/Cu as a electrode) and compare its performance with the obtained simulated results.

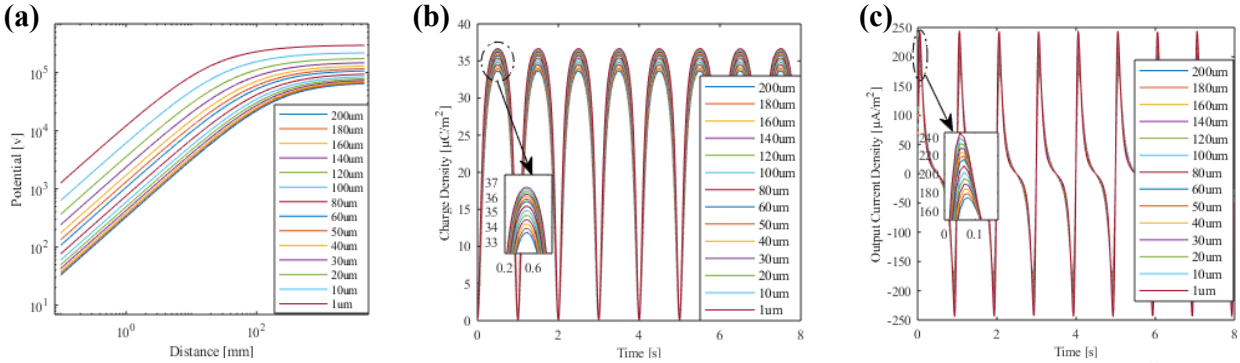

Figure 4. (a) Open circuit voltage vs separation distance (b) Short circuit charge density vs time and (c) Short circuit current density vs time at different thicknesses of PTFE substrate (at 1mm separation height).

REFERENCES

[1] J. McWhorter, L. Brown, and L. Khansa, "A wearable health monitoring system for posttraumatic stress disorder," Biologically Inspired Cognitive Architectures, vol. 22, pp. 44-50, 2017.

[2] D. Wen, X. Zhang, and J. Lei, "Consumers' perceived attitudes to wearable devices in health monitoring in China: A survey study," Computer methods and programs in biomedicine, vol. 140, pp. 131-137, 2017.

[3] R. S. Dahiya, "Epidermal Electronics: Flexible Electronics for Biomedical Application" in , Cambridge University Press, pp. 245-255, 2015.

[4] N. M. Farandos, A. K. Yetisen, M. J. Monteiro, C. R. Lowe, and S. H. Yun, "Contact lens sensors in ocular diagnostics," Advanced healthcare materials, vol. 4, no. 6, pp. 792-810, 2015.

[5] W. Taube Navaraj et al., "Nanowire FET Based Neural Element for Robotic Tactile Sensing Skin," Frontiers in neuroscience, vol. 11, p. 501, 2017.

[6] S. Luo, J. Bimbo, R. Dahiya, and H. Liu, "Robotic tactile perception of object properties: A review," Mechatronics, vol. 48, pp. 54-67, 2017.

[7] C. G. Núñez, W. T. Navaraj, E. O. Polat, and R. Dahiya, "Energy‐Autonomous, Flexible, and Transparent Tactile Skin," Advanced Functional Materials, vol. 27, no. 18, 2017.

[8] R. Dahiya, M. Valle Robotic tactile sensing: Technology and System. USA, NY, New York:Springer-Verlag, pp. 1-245, 2013.

[9] M. Simić, L. Manjakkal, K. Zaraska, G. M. Stojanović, and R. Dahiya, "TiO 2-Based Thick Film pH Sensor," IEEE Sensors Journal, vol. 17, no. 2, pp. 248-255, 2017.

[10] C. Garcia Nunez, W. T. Navaraj, F. Liu, D. Shakthivel, and R. Dahiya, "Large-Area Self-Assembly of Silica Microspheres/Nanospheres by Temperature-Assisted Dip-Coating," ACS applied materials & interfaces, vol. 10, no. 3, pp. 3058-3068, 2018.

[11] S. Khan, R. S. Dahiya, and L. Lorenzelli, "Flexible thermoelectric generator based on transfer printed Si microwires," in Solid State Device Research Conference (ESSDERC), 2014 44th European, 2014, pp. 86-89: IEEE.

[12] R. S. Dahiya, M. Valle, G. Metta, and L. Lorenzelli, "SPICE model of lossy piezoelectric polymers," in Applications of Ferroelectrics, 2008. ISAF 2008. 17th IEEE International Symposium on the, 2008, vol. 3, pp. 1-4: IEEE.

[13] F.-R. Fan, Z.-Q. Tian, and Z. L. Wang, "Flexible triboelectric generator," Nano energy, vol. 1, no. 2, pp. 328-334, 2012.

[14] S. Wang, L. Lin, and Z. L. Wang, "Triboelectric nanogenerators as self-powered active sensors," Nano Energy, vol. 11, pp. 436-462, 2015.

[15] Y. Liu et al., "Integrating a Silicon Solar Cell with a Triboelectric Nanogenerator via a Mutual Electrode for Harvesting Energy from Sunlight and Raindrops," ACS nano, vol. 12, no. 3, pp. 2893-2899, 2018.

[16] T. Bu et al., "Stretchable Triboelectric–Photonic Smart Skin for Tactile and Gesture Sensing," Advanced Materials, vol. 30, no. 16, p. 1800066, 2018.

[17] X. Cheng, B. Meng, X. Zhang, M. Han, Z. Su, and H. Zhang, "Wearable electrode-free triboelectric generator for harvesting biomechanical energy," Nano Energy, vol. 12, pp. 19-25, 2015.

[18] Z. Wang, L. Lin, J. Chen, S. Niu and Y. Zi, Triboelectric nanogenerators, Switzerland, pp.1-537, 2016.

[19] S. Naik, R. Mukherjee, and B. Chaudhuri, "Triboelectrification: A review of experimental and mechanistic modeling approaches with a special focus on pharmaceutical powders," International journal of pharmaceutics, vol. 510, no. 1, pp. 375-385, 2016.

[20] S. Matsusaka, H. Maruyama, T. Matsuyama, and M. Ghadiri, "Triboelectric charging of powders: A review," Chemical Engineering Science, vol. 65, no. 22, pp. 5781-5807, 2010.

[21] A. Kahn, "Fermi level, work function and vacuum level," Materials Horizons, vol. 3, no. 1, pp. 7-10, 2016.

[22] P. Vasandani, Z.-H. Mao, W. Jia, and M. Sun, "Relationship between triboelectric charge and contact force for two triboelectric layers," Journal of Electrostatics, vol. 90, pp. 147-152, 2017.

[23] Y. S. Zhou et al., "Manipulating nanoscale contact electrification by an applied electric field," Nano letters, vol. 14, no. 3, pp. 1567-1572, 2014.

[24] H. Ryu et al., "High‐Performance Triboelectric Nanogenerators Based on Solid Polymer Electrolytes with Asymmetric Pairing of Ions," Advanced Energy Materials, vol. 7, no. 17, 2017.

[25] Y. Wang, Y. Yang, and Z. L. Wang, "Triboelectric nanogenerators as flexible power sources," npj Flexible Electronics, vol. 1, no. 1, p. 10, 2017.

[26] S. Wang et al., "Maximum Surface Charge Density for Triboelectric Nanogenerators Achieved by Ionized‐Air Injection: Methodology and Theoretical Understanding," Advanced Materials, vol. 26, no. 39, pp. 6720-6728, 2014.

[27] S. Niu et al., "Theoretical study of contact-mode triboelectric nanogenerators as an effective power source," Energy & Environmental Science, vol. 6, no. 12, pp. 3576-3583, 2013.

[28] X.-S. Zhang, M. Han, B. Kim, J.-F. Bao, J. Brugger, and H. Zhang, "All-in-One Self-Powered Flexible Microsystems Based on Triboelectric Nanogenerators," Nano Energy, 2018.

[29] M. Parvez Mahmud, N. Huda, S. H. Farjana, M. Asadnia, and C. Lang, "Recent Advances in Nanogenerator‐Driven Self‐Powered Implantable Biomedical Devices," Advanced Energy Materials, vol. 8, no. 2, p. 1701210, 2018.

[30] R. D. I. G. Dharmasena et al., "Triboelectric nanogenerators: providing a fundamental framework," Energy & Environmental Science, vol. 10, no. 8, pp. 1801-1811, 2017.

[31] R. Dharmasena, K. Jayawardena, C. Mills, R. Dorey, and S. Silva, "A unified theoretical model for Triboelectric Nanogenerators," Nano Energy, vol. 48, pp. 391-400, 2018.

[32] J. Walker, Halliday & Resnick fundamentals of physics. Hoboken: Wiley, pp. 1-1450, 2014.